CO_2 flux measurements in volcanic areas using the dynamic concentration method: Influence of soil permeability

M. Camarda,[1] S. Gurrieri,[1] and M. Valenza[2]

Received 23 June 2005; revised 16 January 2006; accepted 30 January 2006; published 20 May 2006.

[1] In order to evaluate the influence of soil permeability on soil CO_2 flux measurements performed with the dynamic concentration method, several tests were carried out using soils characterized by different permeability values and flow rates. A special device was assembled in the laboratory to create a one-dimensional gas flow through a soil of known permeability. Using the advective-diffusion theory, a physical model to predict soil concentration gradients was also developed. The calculated values of CO_2 concentrations at different depths were compared with those measured during the tests and a good agreement was found. Four soils with different gas permeability (3.6×10^{-2} to 1.23×10^{2} μm^2) were used. The CO_2 flux values were varied from 0.1 kg m^{-2} d^{-1} up to 22 kg m^{-2} d^{-1}. On the basis of these results, a new empirical equation for calculating very accurate soil CO_2 flux from dynamic concentration and soil permeability values was proposed. As highlighted by the experimental data, the influence of soil permeability on CO_2 flux measurements depends on various factors, of which the flow rate of the suction pump is the most important. Setting low values for the pumping flux (0.4–0.8 L min^{-1}), the mean error due to soil permeability was lower than 5%. Finally, the method was tested by measuring the CO_2 flux in a grid of 48 sampling sites on Vulcano (Aeolian Islands, Italy), and the global error, affecting the CO_2 flux measurements in a real application, was evaluated.

Citation: Camarda, M., S. Gurrieri, and M. Valenza (2006), CO_2 flux measurements in volcanic areas using the dynamic concentration method: Influence of soil permeability, *J. Geophys. Res.*, *111*, B05202, doi:10.1029/2005JB003898.

1. Introduction

[2] Soil gas emissions are widely used in many research fields such as earthquake forecasting, the evaluation of gas hazard in volcanic areas and geochemical investigations of active faults [*Allard et al.*, 1991; *Badalamenti et al.*, 1988, 1991; *Diliberto et al.*, 1993; *Giammanco et al.*, 1998; *Chiodini and Frondini*, 2001; *Gerlach et al.*, 2001; *Ciotoli et al.*, 2003]. Periodic measurements of soil gas emissions from active volcanoes can be very useful in monitoring the change in volcanic activity, and many research and surveillance projects based on their measurements are in progress in several areas of the world [*Wakita*, 1996; *Ciotoli et al.*, 1998; *Guerra and Lombardi*, 2001; *Rogie et al.*, 2001; *Spicák and Horálek*, 2001; *Salazar et al.*, 2002]. These studies are mainly focused on measuring CO_2 flux, the most abundant volatile species in magma after water and, at the same time, one of the less soluble species. During the magma ascent toward the surface, diffuse soil CO_2 is therefore one of the geochemical parameters that can be affected by significant variations.

[3] The gas flux through a natural soil is the result of two different processes: diffusion and advection [*Sahimi*, 1995]. Molecular diffusion is the process where a gas species is transported from a region of high concentration to a region of low concentration, as the result of random molecular movement. Advection is the process where a gas mixture, or a single gas species, is transported in response to a pressure gradient. In a natural context, gas transport occurs by a combination of these two different processes and the total flux is the sum of the advective and the diffusive component. Generally, low flux values are associated with diffusion, whereas high values occur when advection is the prevalent gas transport modality [*Gurrieri and Valenza*, 1988].

[4] CO_2 flux measurements can be performed using both indirect and direct methods. The calculation of the CO_2 flux from the concentration gradients in the soil is an example of an indirect method [*Baubron et al.*, 1990]. In this case, the flux values are calculated according to the one-dimensional steady state model of gas transport through a homogeneous porous medium. This methodology requires the knowledge of some soil properties, such as air-filled porosity, tortuosity and permeability, which are generally difficult to determine. Other methods have been developed with which to perform more accurate and rapid flux measurements. Some of these are based on the absorption of CO_2 in a caustic solution (alkali adsorption method [*Witkamp*, 1966; *Kirita*, 1971; *Anderson*, 1973]) and on the measurement of the difference

[1] Istituto Nazionale di Geofisica e Vulcanologia, Palermo, Italy.
[2] Dipartimento di Chimica e Fisica della Terra ed Applicazioni, Palermo, Italy.

0148-0227/06/2005JB003898$09.00

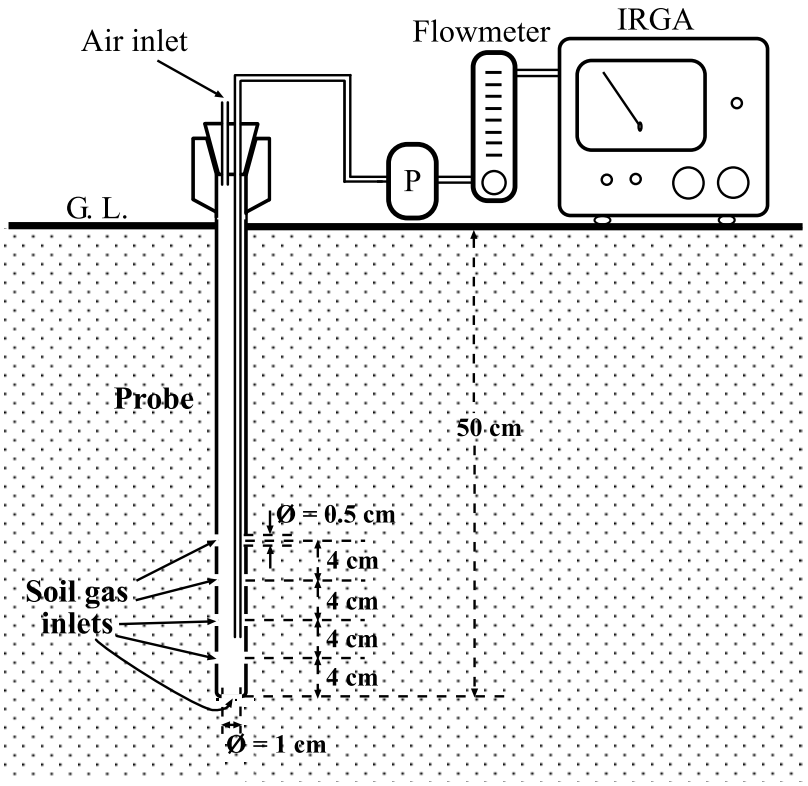

Figure 1. Schematic illustration of the system used for measuring soil CO_2 flux. P, sampling pump; G.L., ground level; IRGA, infrared gas analyzer.

in CO_2 concentrations between inlet and outlet air in a closed chamber (open flow infrared gas analysis [*Witkamp and Frank*, 1969; *Nakadai et al.*, 1993]). In volcanological and geothermal studies, the most widespread methods for measuring soil CO_2 fluxes are the accumulation chamber [*Tonani and Miele*, 1991; *Bekku et al.*, 1955; *Norman et al.*, 1992; *Chiodini et al.*, 1998] and the measurement of dynamic concentration [*Gurrieri and Valenza*, 1988; *Giammanco et al.*, 1995]. The first method is based on the CO_2 accumulation rate inside an open box (the chamber) of known volume. The measurement is performed at ground level and the flux value is calculated by a theoretical equation, according to the volume, pressure and temperature values of the chamber atmosphere.

[5] The dynamic concentration method has been used in several field applications since 1988 [*Badalamenti et al.*, 1988; *Diliberto et al.*, 2002; *De Gregorio et al.*, 2002; *Giammanco et al.*, 1995, 1998]. This method has been principally applied to the monitoring of volcanic activity and in the study of the relationship between soil degassing and tectonics. The dynamic concentration method consists of measuring the CO_2 content in a mixture of air and soil gas (C_d), which has been obtained by a special probe (Figure 1). As deduced by *Gurrieri and Valenza* [1988], the dynamic concentration is proportional to the soil CO_2 flux according to an empirical relationship, which was experimentally found for CO_2 flux values ranging between 0.44 and 9.2 kg m^{-2} d^{-1} and a soil characterized by a permeability of 24 μm^2. The error in the flux measurements referred to different working conditions from those above indicated, such as different soil permeability and different flux values was not known.

[6] Starting from these considerations a new apparatus for simulating a natural degassing system under known laboratory conditions was developed and several measurements were taken using dynamic concentration method in order to clarify the influence of soil permeability on the CO_2 flux measurements. The soil CO_2 fluxes explored in this work range from 0.1 to 22 kg m^{-2} d^{-1}, and they cover more than the natural flux range normally observed in volcanic and geothermal areas. The permeability values of the media used in the laboratory experiments varied by 4 orders of magnitude (from 3.6×10^{-2} to 1.23×10^{2} μm^2); various important characteristics of the measurement system, such as the pumping flux, were also systematically varied during the tests in order to define the most suitable operating conditions for measuring CO_2 flux from the soil with the dynamic concentration method.

[7] In this paper, the results of the laboratory tests will be presented and a new empirical relationship between the dynamic concentration, the soil permeability and the soil CO_2 flux will be proposed. This relationship allows more accurate CO_2 flux measurements. Finally, the results of some soil CO_2 flux and permeability surveys performed in a volcanic area (Vulcano, Aeolian Islands, Italy) are discussed in order to evaluate the errors in a real field application.

2. Generalities Regarding the Dynamic Concentration Method

[8] The system developed for measuring CO_2 flux from soils is schematically shown in Figure 1. The main components are an infrared gas analyzer (IRGA), a pump and a

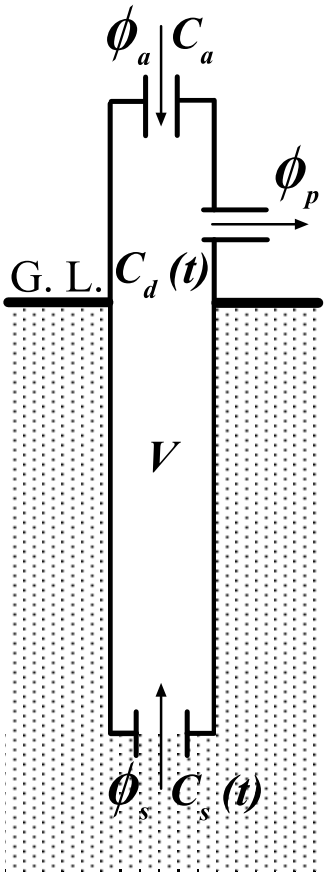

Figure 2. Simplified diagram of the probe used for measuring soil CO_2 flux. V is the inner volume of the probe; $C_d(t)$ is the CO_2 concentration of the gas-air mixture; ϕ_a and C_a are the volumetric flux and CO_2 concentration in the inlet air, respectively; ϕ_s and C_s (t) are the volumetric flux and CO_2 concentration (the static concentration) in the sucked soil gas, respectively; ϕ_p is the volumetric pumping flux; G.L., ground level.

probe which is inserted into the soil at a depth of 0.5 m. Soil gases and air can drain inside the probe through openings located on the lower part of the probe and a calibrated tube on the top, respectively. By pumping at constant flux, an air and soil gas mixture is obtained inside the probe and, after a given time, depending on the pumping flux and probe geometry, this gas mixture reaches a constant composition. *Gurrieri and Valenza* [1988] defined as dynamic (C_d) the concentration values obtained by this method to distinguish them from the static gas concentrations in soils (which are generally measured to determine the soil concentration gradients). The same authors observed that the dynamic concentration of CO_2 is mainly a function of soil CO_2 flux (J_{CO_2}) according to the relationship

$$J_{CO_2} = KC_d \tag{1}$$

where C_d is the dynamic concentration of CO_2 and K is a constant, depending on the geometry of the probe, the soil insertion depth, the pump flux and the soil permeability.

[9] A theoretical expression for the dynamic concentration can be deduced by making a mass balance between the CO_2 inlet and outlet in the probe. Figure 2 shows a scheme of the probe, where all the lower openings of the sampling probe have been assimilated into a single opening. The CO_2 mass change within the probe, $dM_{CO_2}(t)$, can be expressed as the difference between the CO_2 entering the probe (from the soil and atmosphere) and the CO_2 outgoing from the probe (to the IRGA) in a prefixed time interval, dt:

$$dM_{CO_2}(t) = VdC_d(t) = \phi_a C_a dt + \phi_s C_s(t)dt - \phi_p C_d(t)dt \tag{2}$$

where V [L^3] is the inner volume of the probe; $C_d(t)$ [M L^{-3}] is the CO_2 concentration of the gas mixture inside the probe at time t; ϕ_a [L^3 T^{-1}] and C_a [M L^{-3}] are the volumetric flux and CO_2 concentration in the air entering the probe, respectively; ϕ_s [L^3 T^{-1}] and $C_s(t)$ [M L^{-3}] are the volumetric flux and CO_2 concentration in the soil gas entering the probe, respectively; $C_s(t)$ [M L^{-3}] is the CO_2 concentration of the soil gas entering the probe at time t; ϕ_p [L^3 T^{-1}] is the volumetric pumping flux. Assuming that $C_a = 0$ and C_s remains constant during the necessary time for reaching a steady state, $C_s(t) = C_s$, a first-order homogeneous differential equation for $C_d(t)$ can be developed:

$$\frac{dC_d(t)}{dt} + \frac{\phi_p}{V} C_d(t) = \frac{\phi_s C_s}{V},$$

whose the general solution is

$$C_d(t) = \frac{\phi_s}{\phi_p} C_s \left(1 - ae^{-(\phi_p/V)t}\right), \tag{3}$$

where a is a constant and it can be calculated by assuming that C_d at $t = 0$ is equal to the concentration of the soil gas

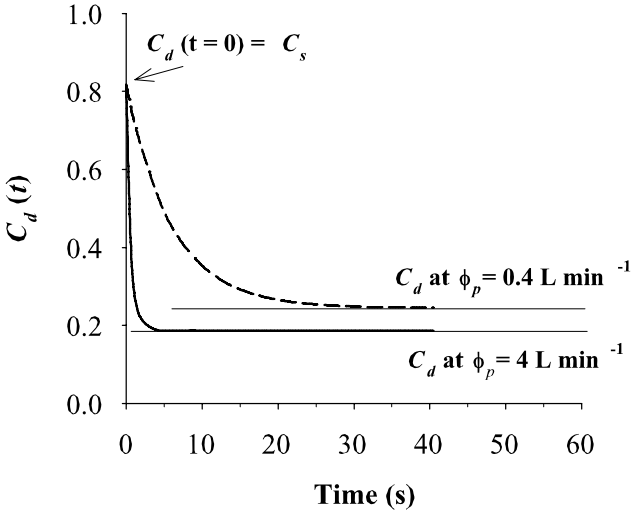

Figure 3. Theoretical variation in the gas mixture concentration $C_d(t)$ versus time for two different values of pumping flux: solid line, 4 L min^{-1}; dashed line, 0.4 L min^{-1}.

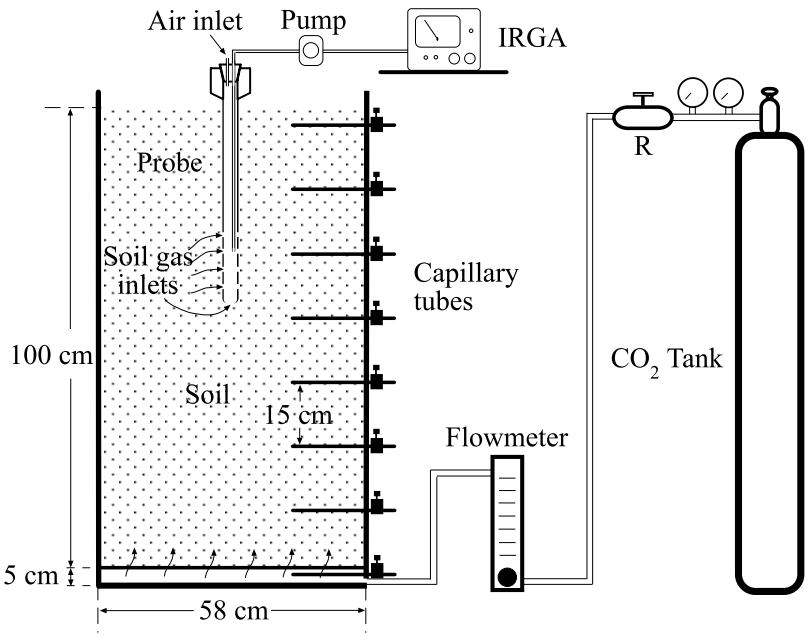

Figure 4. Schematic illustration of the apparatus used in the laboratory for simulating CO_2 transport through a soil layer of known permeability. This consists of a cylindrical metallic container, 0.58 m in diameter, fed by a known flux of CO_2 at the bottom; sampling capillary steel tubes inserted at different depths in soil. The capillaries for studying soil CO_2 transport are placed 0.15 m from each other, and they are hermetically sealed by spherical valves. The probe for measuring dynamic concentration was inserted at 50 cm depth in the soil layer.

entering the probe, $C_d(0) = C_s$. According to the specified boundary conditions, equation (3) becomes

$$C_d(t) = \frac{\phi_s}{\phi_p} C_s \left(1 - \frac{\phi_s - \phi_p}{\phi_s} e^{-(\phi_p/V)t}\right) \quad (4)$$

Equation (4) shows the temporal variation in the CO_2 concentration of the gas mixture inside the probe by pumping at constant flux. By using this equation, the necessary time for reaching steady state can be calculated. Figure 3 shows the theoretical $C_d(t)$ values versus time at different values of pumping flux, calculated by equation (4) when $C_s = 82$ vol %, $\phi_s = 1$ L min^{-1} and $V = 2.3 \times 10^{-3}$ m^3 (inner volume of the probe). In each case, the concentration of the gas mixture decreases as a function of time from C_s to C_d. The time necessary for reaching a steady state ranges from between 5 s for high values of pumping flux (4 L min^{-1}) and 25 s for lower flux values (0.4 L min^{-1}). As confirmed by experimental observations, the theoretical values represent the minimum time necessary to carry out the C_d measurement because the model does not take into account various geometrical aspects, such as the length of the tube between the probe and the IRGA and the volume of the IRGA measurement cell. These discrepancies can range from between 5 s (for a $\phi_p = 4$ L min^{-1}) and 60 s ($\phi_p = 0.4$ L min^{-1}).

[10] At steady state ($t \rightarrow \infty$), the concentration of each gas species in the gas mixture becomes constant and equal to the limit for $t \rightarrow \infty$, of equation (4):

$$C_d(t \rightarrow \infty) = \frac{\phi_s}{\phi_p} C_s \quad (5)$$

C_d does not depend on the inner volume of the probe (V), whereas it is only a function of the pumping flux (ϕ_p) and the flux and CO_2 concentration of the soil gas entering the probe (ϕ_s and C_s). Moreover, for ϕ_p = const, C_d is only a function of C_s and ϕ_s.

[11] The starting assumptions are quite reasonable. As confirmed by several measurements, C_s decreases appreciably only for high values of pumping flux and after several minutes of pumping time (for $\phi_p = 4$ L min^{-1}, the C_s decrement is less than 2% and 8% after 5 and 20 min, respectively). At the measuring conditions fixed for this method ($\phi_p = 0.8$ L min^{-1} and pumping time <1 min) the C_s decrement is sensibly lower than the measurement error.

3. Laboratory Experiments

[12] The relationship between C_d and J_{CO_2} is a very complex function which involves both the geometry of the probe and the properties of the soil. To investigate this relationship, several C_d measurements were performed in the laboratory by simulating different soil gas regimens, using an apparatus very similar to that described by *Gurrieri and Valenza* [1988] (Figure 4). It consists of 700 kg of soil which was stored in a cylindrical vessel, 0.58 m in diameter. The soil layer (1 m high) was supported by a perforated disk 0.05 m off the bottom. Furthermore, eight sampling capillary tubes were inserted at different depths in the soil through which the CO_2 concentrations could be measured. Pure CO_2 (99.99%) was admitted at the base of soil layer with a constant flux. The flux rate was measured using three in-line flowmeters with different full scale and sensibility, in order to keep an high accuracy (<3%) in all investigated range of CO_2 fluxes (0.1–22 kg m^{-2} d^{-1}).

Table 1. Main Physical Characteristics of the Soil Samples Used in the Laboratory

Soil Sample	k, μm^2	Porosity, %	Tortuosity Factor, τ	Bulk Diffusion Coefficient D, $m^2\ s^{-1}$
S_1	123 ± 7	39	1.38	4.5×10^{-6}
S_2	36 ± 2	38	1.39	4.4×10^{-6}
S_3	5.5 ± 0.7	34	1.41	3.8×10^{-6}
S_4	0.36 ± 0.02	28	1.46	3.0×10^{-6}

[13] In order to study and define the relationship between C_d and J_{CO_2} at constant permeability, thirteen C_d measurements at thirteen different CO_2 fluxes were carried out in a soil characterized by a permeability equal to 123 μm^2 (S_1 soil sample). Successively, the measurements were repeated using soils characterized by different gas permeability. As total, four different soils were used in these experiments (S_1, S_2, S_3, and S_4 soil samples). The principal physical properties of these soil samples are reported in Table 1.

[14] The gas permeability values (k) of each soil sample were obtained by measuring the pressure gradient in the soil which was generated by different air fluxes (v), according to the one-dimensional form of Darcy's law [*Scheidegger*, 1974]:

$$v = -\frac{k}{\mu}\frac{P_L^2 - P_0^2}{2LP_L}$$

where μ is the air viscosity, k is the intrinsic gas permeability, L is the thickness of the soil layer, P_L and P_0 are the gas pressure measured at 0 and L depths, respectively (in this case, the soil surface in contact with the gas source was assumed as 0 depth). The permeability of the each soil sample was measured after the sample was placed inside the cylindrical vessel. The P_L and P_O pressure measurements were carried out using a digital differential manometer (accuracy of 1 Pa), which was connected to the capillary tubes of the simulation system (Figure 4). The measurements were carried out under low-pressure conditions ranging between 10 and 600 Pa m^{-1} in order to reproduce the pressure gradients which can be normally measured in active volcanic areas (<320 Pa m^{-1} [*Natale et al.*, 2000]). In this pressure range, the deviation induced by Klinkenberg's effect is very small and less than the measurement errors. According to Klinkenberg's equation [*Klinkenberg*, 1941], the absolute permeability values measured using a gas flux are significantly different from those measured in the same soil using water. However, the values discussed in this paper are more useful and reliable to discuss and model soil gas transfers.

[15] S_1 and S_2 soil samples were obtained by grain size separation of pyroclastic sand which had been collected close to the isthmus of the island of Vulcano (Aeolian Archipelagos, Italy). The S_1 grain size ranged between 5×10^{-4} and 1×10^{-3} m, while it was smaller than 5×10^{-4} m for the S_2 sand. According to the *Wentworth* [1922] classification, the S_1 sample is coarse sand while S_2 is fine sand. The S_4 sample was a limestone powder produced by the industrial processing of marble. Finally, the S_3 sample was obtained in the laboratory by mixing seven parts of S_1 with three parts of S_4. These artificial soils resulted both homogeneous and stable in time, two necessary conditions for the calibration purposes of this work. The gas permeability of the investigated soils varied by 4 orders of magnitude (Table 1). The values of gas permeability measured in situ by other authors [*Evans and Kirkham*, 1949; *Grover*, 1955] and those discussed in this work fall inside this range. Unfortunately, there are not others available data in the literature because they generally refer to liquid permeability and, due to the Klinkenberg effect, cannot be directly compared.

[16] To simulate a real soil gas regimen, pure CO_2 was injected through the soil layer at a constant and known flux. At the beginning of each test, the soil gas in each layer consisted exclusively of air at atmospheric pressure. As CO_2 entered the soil, the CO_2 concentrations at different depths increased with variable rates until steady state was reached. For each test, these variations were monitored by sampling the soil gas at different depths using the capillary tubes. Figure 5 shows the CO_2 concentrations measured at various depths versus time for a test, where $J_{CO_2} = 0.34$ kg m^{-2} d^{-1} and $k = 123$ μm^2. A steady state for these specific boundary conditions was reached after 28 hours; before it was reached, the CO_2 flux admitted at the base of the soil was

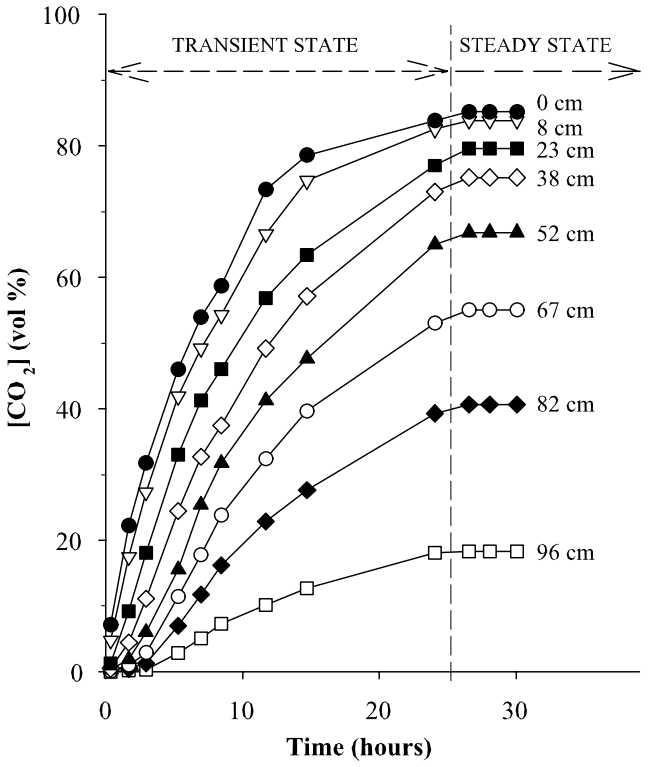

Figure 5. Temporal variations in soil CO_2 concentrations at different depths (k = 123 μm^2 and J_{CO_2} = 0.34 kg m^{-2} d^{-1}).

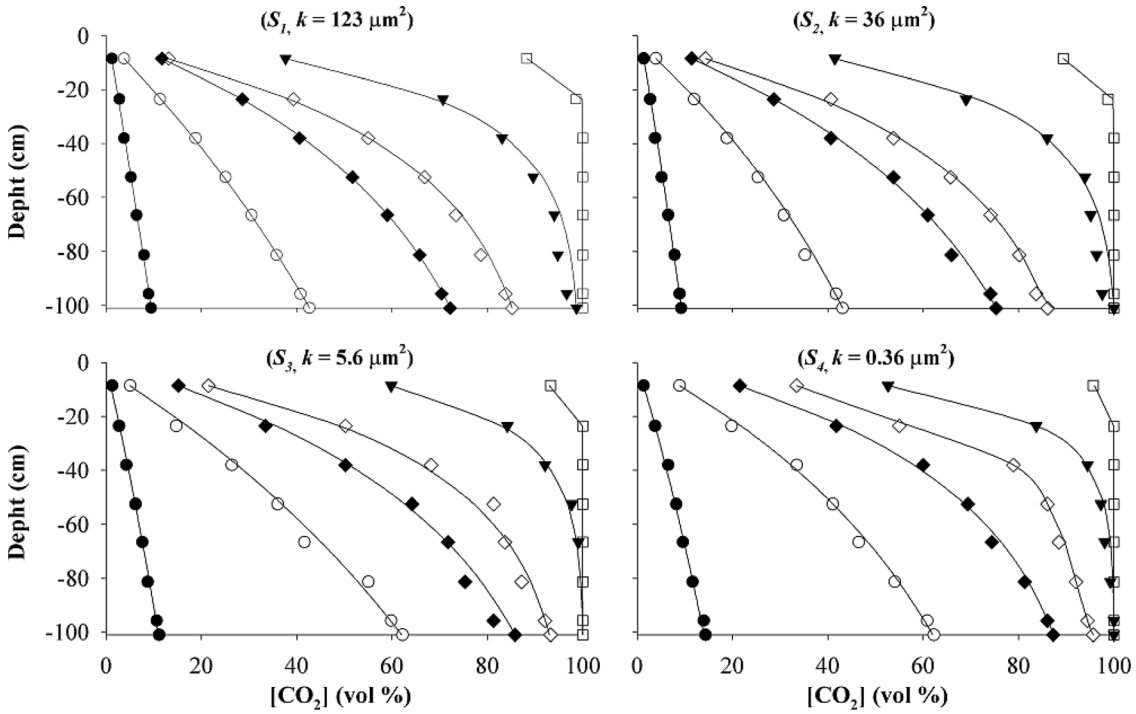

Figure 6. Experimental (symbols) and theoretical (lines) CO_2 concentration profiles of six different J_{CO_2}, for each investigated soil sample (S_1, S_2, S_3 and S_4): solid circles, J_{CO_2} = 0.1 kg m^{-2} d^{-1}; open circles, J_{CO_2} = 0.5 kg m^{-2} d^{-1}; solid diamonds, J_{CO_2} = 1.2 kg m^{-2} d^{-1}; open diamonds, J_{CO_2} = 2.4 kg m^{-2} d^{-1}; solid triangles, J_{CO_2} = 3.5 kg m^{-2} d^{-1}; open squares, J_{CO_2} = 22 kg m^{-2} d^{-1}.

higher than the CO_2 flux released by the system into the atmosphere. The difference between the two CO_2 amounts was stored inside the soil and it determined the increase in the CO_2 concentration at various depths. When the steady state had been reached the CO_2 flux inlet was equal to the CO_2 flux outlet.

[17] Thirteen different CO_2 fluxes ranging from 0.1 up to 22 kg m^{-2} d^{-1} were investigated. Within this range, the CO_2 transport regimen in the soil changes from mainly diffusive (where the CO_2 flux is mainly driven by concentration gradient) to mainly advective (where the CO_2 flux is mainly driven by pressure gradient). The imposed fluxes maintained through the soil samples were little higher than those normally measured in soil respiration studies (3.6×10^{-3} to 14×10^{-3} kg m^{-2} d^{-1} [*Monteith et al.*, 1964]; 3.4×10^{-3} to 56×10^{-3} kg m^{-2} d^{-1} [*Lunderghard*, 1927]), but they were within the range of CO_2 fluxes which are normally encountered in active volcanoes and geothermal areas [*Badalamenti et al.*, 1991; *Chiodini et al.*, 1998; *Diliberto et al.*, 2002].

[18] Figure 6 shows some examples of the experimental concentration profiles obtained for each soil sample at different J_{CO_2}. The CO_2 profiles are linear at low J_{CO_2} but they curve progressively at higher fluxes. As suggested by *Gurrieri and Valenza* [1988], this trend represents the change from conditions where CO_2 transport is dominated by diffusion to conditions dominated by advection. Figure 6 shows the theoretical profiles (solid lines) calculated according to the equation (Appendix A):

$$C_{CO_2}(z) = C_0 + \frac{(C_L - C_0)}{(e^{(v/D)L} - 1)}\left(e^{(v/D)z} - 1\right) \quad (6)$$

This equation was deduced from the one-dimensional form of the advective-diffusion equation [*Isachenko et al.*, 1980; *Sahimi*, 1995] where C_L and C_0 are the CO_2 concentration of soil gas measured at depth of 0 and L, respectively, z is the depth, v is the measured advective gas flux and D is the bulk diffusion coefficient expressed by the following relation:

$$D = \frac{D_m n}{\tau}$$

where D_m is the molecular diffusion coefficient of CO_2 in air, n is experimental air-filled porosity and τ is the tortuosity value relative to each soil sample (Table 1). The D_m value at T_0 = 273.2 K at P_0 = 1.013 ($D_{m,(STP)}$) is equal to 1.39×10^{-5} m^2 s^{-1} Pa. The D_m value used in the [CO_2] calculation under other conditions of temperature, T and pressure, P, was estimated from this relation [*Campbell*, 1985]:

$$D_m = D_{m,(STP)}\left(\frac{T}{T_0}\right)^{1.75}\left(\frac{P_0}{P}\right)$$

The tortuosity factor is defined as the ratio of the effective path length to the linear sample length and it was calculated from the relation [*Fang and Moncrieff*, 1999]

$$\frac{n}{\tau} = n^{2a}\left(\frac{n}{n_t}\right)^2$$

where n_t is the total porosity of the medium (air and water filled porosity) and a is an empirical coefficient

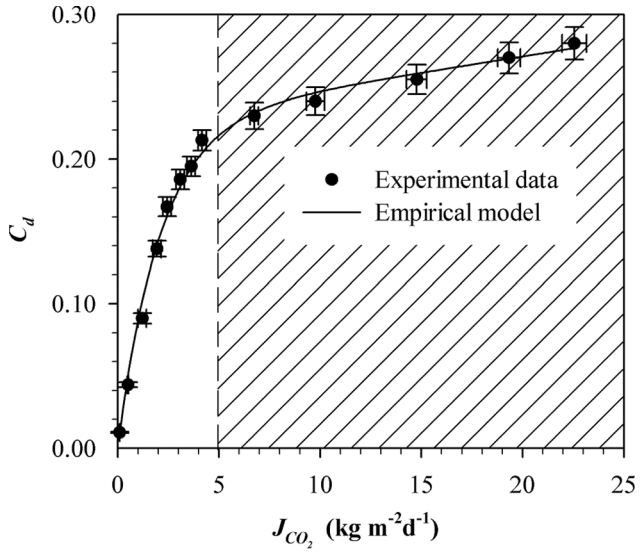

Figure 7. Relationship between C_d and J_{CO_2} at constant soilpermeability (k = 123 μm^2) and pumping flux (ϕ_p = 4 L min^{-1}). The symbols represent experimental values (error bars are also reported). The solid line shows the best fitting curve, calculated according to equation (8). The dashed area indicates the range of J_{CO_2} where CO_2 flux is mainly driven by advection. C_d values are expressed as molar fraction.

determined from the relation [*Millington and Shearer*, 1971]

$$n^{2a} + (1 - n)^a = 1$$

As suggested by Figure 6, a good agreement was found between the theoretical and the experimental soil

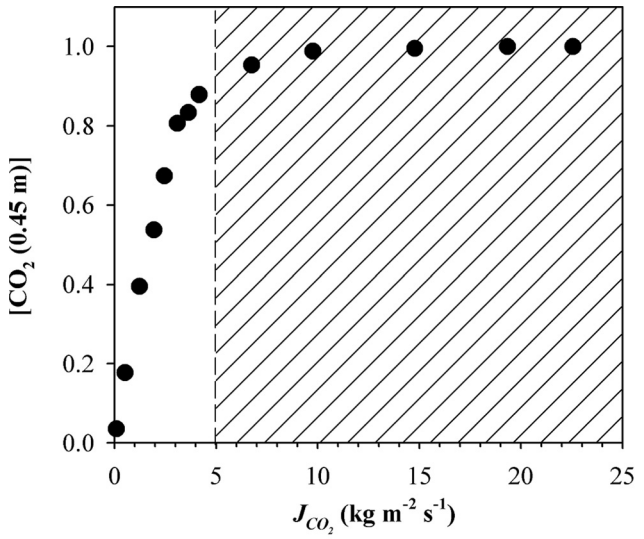

Figure 8. CO_2 concentration [CO_2 (0.45 m)] measured at a depth of 0.45 m in the S_1 soil sample as a function of J_{CO_2}. The dashed area indicates the range of J_{CO_2} where CO_2 flux is mainly driven by advection.

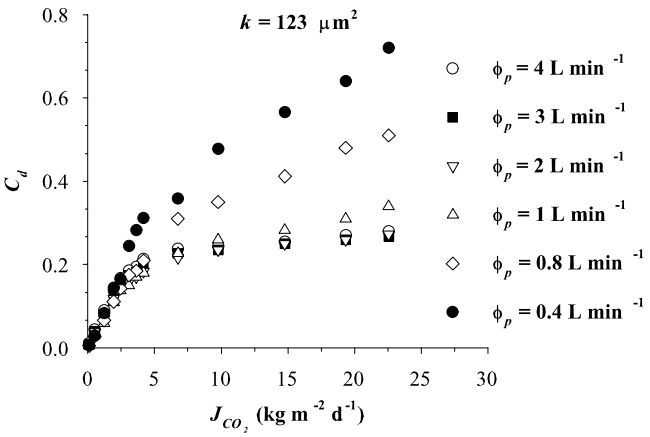

Figure 9. Relationship between C_d and J_{CO_2} for each investigated pumping flux and a constant soil permeability (k = 123 μm^2). C_d values are expressed as molar fraction.

CO_2 profiles for each permeability and explored CO_2 flux.

4. Results and Discussions

4.1. Experimental Conditions

[19] In order to test the dynamic concentration method, the measurement probe of Figure 1 was inserted at 0.5 m depth in the soil of the experimental apparatus described in the previous paragraph (Figure 4). The dynamic CO_2 concentration was measured using a portable IR spectrophotometer and a pump connected to the probe. During all experiments, the probe geometry and the insertion depth in the soil of the measurement probe remained unvaried. The probe employed in these experiments (Figure 1) was characterized by a greater number of openings than the probe used by *Gurrieri and Valenza* [1988]. Indeed, for the same soil flux, a greater CO_2 inlet surface determined a higher amount of soil gas in the gas mixture and, consequently, it provided higher C_d values. This solution was preferred because it determines an increase in sensitivity at the lowest soil CO_2 fluxes.

[20] For each imposed value of CO_2 flow admitted trough the soil layer, several C_d measurement were taken, when steady state had been reached. The experimental conditions can be summed up as follows: J_{CO_2} = 0.1–22 kg m^{-2} d^{-1}, k = 0.36–123 μm^2, pumping flux = 0.4–4 L min^{-1}.

4.2. Laboratory Experiments at Constant Soil Permeability and Pumping Flux

[21] The first set of measurements was performed on soil sample S_1 (k = 123 μm^2) at a constant pumping flux of 4 L min^{-1}. Figure 7 shows the relationship between the measured C_d values (expressed as a molar fraction) and the imposed fluxes (J_{CO_2}). As a first consideration, C_d changes as a linear function of J_{CO_2} at low and high fluxes (J_{CO_2} < 3 kg m^{-2} d^{-1} and J_{CO_2} > 9 kg m^{-2} d^{-1}, respectively). An abrupt change in slope is achieved at J_{CO_2} = 5 kg m^{-2} d^{-1}. This general behavior characterizes also the measurement sets performed at other pumping fluxes and permeability conditions and it represents the transition from a diffusion-

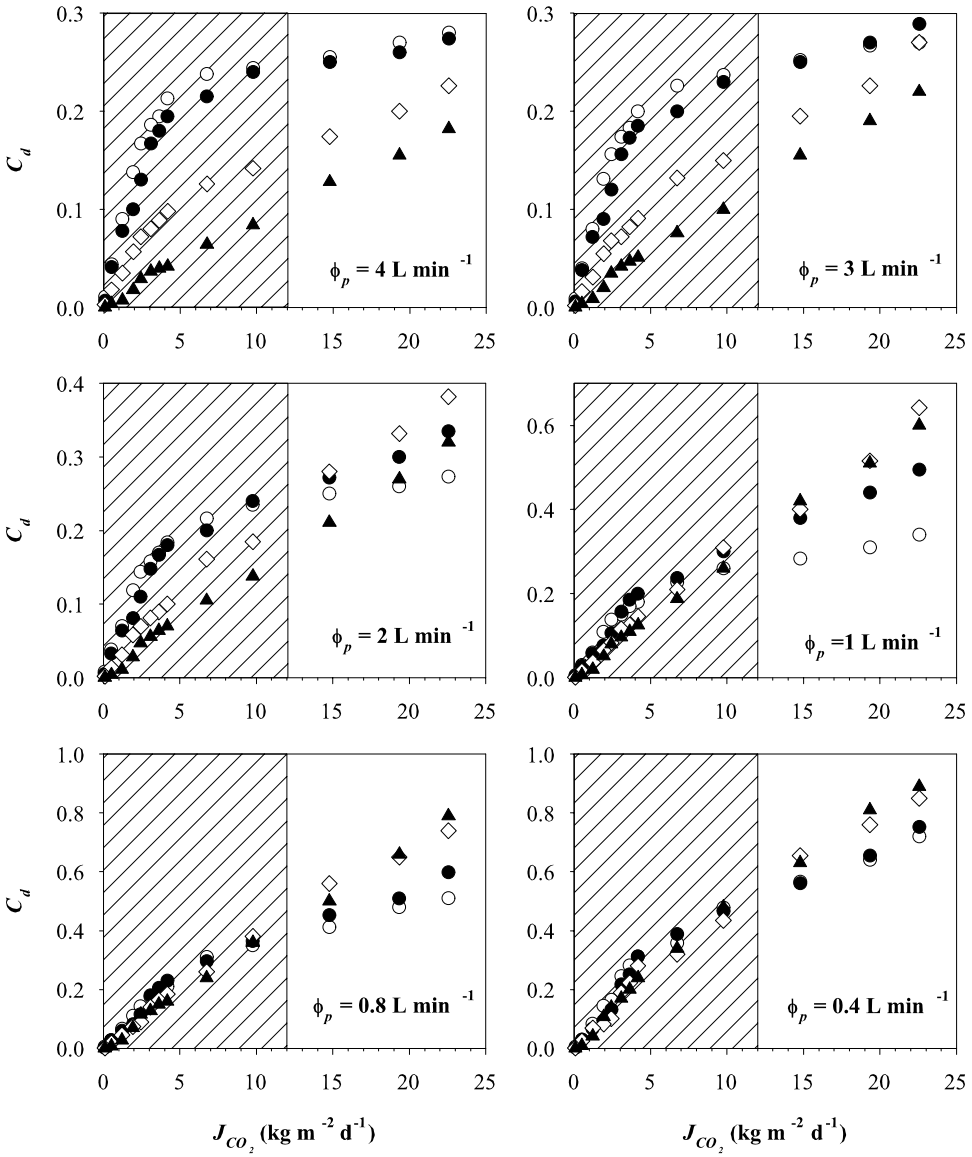

Figure 10. Relationship between C_d and J_{CO_2} for each investigated soil permeability and different pumping fluxes. Open circles, k = 123 μm^2; solid circles, k = 36 μm^2; open diamonds, k = 5.5 μm^2; solid triangles, k = 0.36 μm^2. The dashed area indicates the range of J_{CO_2} which is normally observed in volcanic and geothermal areas. C_d values are expressed as molar fraction.

advective regimen to a pure advective regimen of the soil CO_2 transfer. In the first part of the curve, the C_d/J_{CO_2} slope is sensibly higher because reflects a simultaneously change in soil CO_2 concentration (C_s) and soil gas pressure. In the second part, as suggested by the Figure 8, the soil CO_2 concentration reaches the saturation and C_d/J_{CO_2} slope is only due to the gas pressure variation in the soil.

4.3. Influence of the Pumping Flux (ϕ_p) and the Soil Permeability (k) on the Dynamic Concentration Measurements

[22] In order to investigate the influence of the pumping flux on the relationships between C_d and J_{CO_2}, several C_d measurements were repeated at different values of pumping flux, ranging from 0.4 to 4 L min^{-1}. Figure 9 shows the results of these tests performed on a soil whose permeability was 123 μm^2. Significant discrepancies can be observed between the C_d-J_{CO_2} lines, especially for high J_{CO_2} values, and conversely, small differences are observed at low J_{CO_2} values.

[23] More interesting results are shown in Figure 10, where the experimental relationships between C_d and J_{CO_2} in each soil are compared in relation to different values of the pumping flux. The dashed area in these plots indicates the range of CO_2 flux normally measured in volcanic and geothermal areas (J_{CO_2} < 11 kg m^{-2} d^{-1} [*Badalamenti et al.*, 1991; *Chiodini et al.*, 1998; *Diliberto et al.*, 2002]). Large discrepancies can be observed in relation to different values of soil permeability, especially at higher values of the pumping flux (1–4 L min^{-1}). On the contrary, at low values of the pumping flux (0.4–1 L min^{-1}) and for realistic soil

Table 2. Values of a, b, and c Coefficients[a]

k, μm^2	a, kg m^{-2} d^{-1}	b	c, kg m^{-2} d^{-1}
123	115.8	3.021	14.10
36	59.61	2.949	18.73
5.5	13.21	3.083	23.39
0.36	2.385	3.044	27.58

[a]The a, b, and c values were computed fitting equation (8) to experimental C_d and J_{CO_2} data for a constant pumping flux of 0.8 L min^{-1}.

Table 3. Reproducibility of the Flux Measurements[a]

Site	CO_2 Flux, $\times 10^{-3}$ kg m^{-2} d^{-1} Range	Mean	σ	CV
1	132–139	136.2	3	2%
2	27–30	27.9	1	5%
3	458–475	468.2	9	2%
4	797–831	817.4	13	2%

[a]CO_2 flux measurements (kg m^{-2} d^{-1}) repeated at four sites located close to Grotta dei Palizzi (Vulcano Island, Italy); σ and CV refer to standard deviation and coefficient of variation of the measured data, respectively.

flux values (dashed area), these differences significantly decrease and become negligible.

[24] As suggested by these data, the dependence of the measured CO_2 flux on the soil permeability is a function the pumping flux. At high values of the pumping flux, a high pressure deficit inside the probe is generated (~40 Pa) inducing a forced gas flux from the soil to the probe. This flux is obviously related to the permeability of the soil being measured. In particular, for a fixed pressure deficit between the soil and the probe, the gas flux sucked out from a high permeability and porosity soil will be higher than that from a low permeable soil. This effect strongly decreases at low values of the pumping flux and theoretically disappeared for pumping fluxes close to zero; in this last condition, no pressure deficit between the probe and the soil is generated, and therefore no forced gas flux from the soil is induced. For a pumping flux equal to 0.8 L min^{-1}, the discrepancies caused by the soil permeability are on average less than 5% of the measured absolute value. A lower pumping flux generates lower errors but, at the same time, it determines an increase in the time necessary for performing the C_d measurements. The measurement time was less than 40 s for a pumping flux equal to 0.8 L min^{-1}.

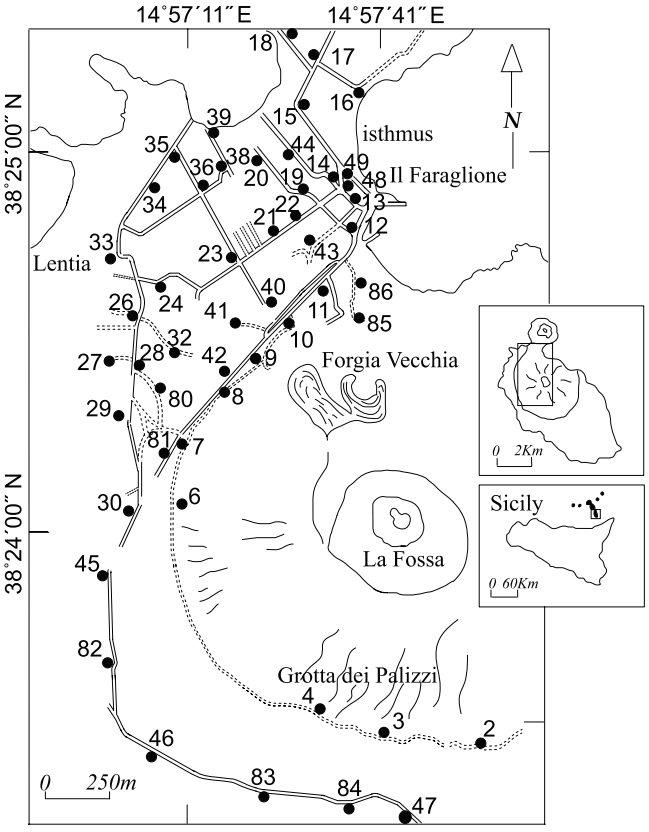

Figure 11. Location of the 48 permeability and flux measurement sites.

4.4. Relationship Between J_{CO_2}, C_d, and Soil Permeability (k)

[25] The relationship between J_{CO_2} and C_d observed at constant soil permeability and at constant pumping flux (see Figure 7) is a very complex function: it is linear for low and high J_{CO_2} and it is not linear for intermediate fluxes. An analytical function capable of describing this relationship can obtained by the sum of the linear and power terms of C_d:

$$J_{CO_2} = cC_d + aC_d^b \tag{7}$$

Fitting this model to the experimental data (Figure 7), a good agreement is found ($R = 0.996$). The values of the a, b, and c coefficients of equation (7) are a function of the soil permeability and the pumping flux. Table 2 reports the values of these coefficients found for each permeability and for a constant pumping flux of 0.8 L min^{-1}. The values of coefficients a and c of equation (7) change as a function of the soil permeability in accordance with a power function ($a = 6.3 \times k^{0.6}$, $b = 32–5.8 \times k^{0.24}$), while the b value was constant and equal to 3. Therefore equation (7) can be modified in order to consider the soil permeability in the CO_2 flux calculation:

$$J_{CO_2} = \left(32 - 5.8k^{0.24}\right)C_d + 6.3k^{0.6}C_d^3 \tag{8}$$

Equation (8) can be used for taking accurate measurements of soil CO_2 flux by measuring the dynamic concentration of CO_2 with a probe whose geometry is indicated in Figure 1 and by setting a pumping flux which is equal to 0.8 L min^{-1} and measuring the soil permeability. Similar expression can be deduced for different pumping fluxes.

4.5. Reproducibility of the Method

[26] Several measurements of soil CO_2 flux were performed in a selected area on Vulcano (Aeolian Islands, Italy), close to Grotta dei Palizzi (Figure 11) to verify the reproducibility of the flux measurements performed with this method. Soil CO_2 flux measurements were repeated ten times at four sites over a 1 hour period. The results of these flux measurements are reported in Table 3 with the some statistical parameters. The reproducibility of this method

Table 4. Soil Permeability and CO_2 Flux Values Measured in the Surveyed Area in the April and June 2003[a]

	k, μm^2		J_{CO_2}, $\times 10^{-3}$ kg m^{-2} d^{-1}		J_{CO_2} (k = 37 μm^2), $\times 10^{-3}$ kg m^{-2} d^{-1}		δ, %	
Sites	April 2003	June 2003	April 2003	June 2003	April 2003	June 2003	April 2003	June 2003
2	50.1	47.7	200	74	215	78	−7	−5
3	33.6	21.4	137	33	137	31	0	6
4	44.6	61.6	2823	524	2928	587	−4	−11
6	25.1	29.1	2	2	2	2	0	0
7	26.0	35.5	12	15	12	16	0	−6
8	40.2	66.4	7	3	7	4	0	−29
9	71.0	71.9	25	14	29	16	−15	−13
10	24.4	35.5	16	15	16	15	0	0
11	32.3	29.1	20	14	20	14	0	0
12	22.3	45.2	249	204	235	215	6	−5
13	44.6	50.6	1476	629	1545	676	−5	−7
14	6.4	28.1	7	159	6	155	15	3
15	44.6	45.2	698	78	733	82	−5	−5
16	53.2	66.4	18	12	20	14	−11	−15
17	19.0	29.1	13	8	12	8	8	0
18	21.1	23.9	13	9	12	9	8	0
19	53.2	61.6	27	122	29	137	−7	−12
20	50.1	35.5	22	23	23	23	−4	0
21	42.4	71.9	28	32	29	37	−4	−14
22	20.0	26.2	15	4	14	4	7	0
23	44.6	57.4	28	21	29	23	−4	−9
24	26.0	34.0	12	8	12	8	0	0
26	16.9	25.4	11	5	10	5	10	0
27	17.3	21.4	11	6	10	6	10	0
28	21.1	25.4	13	8	12	8	8	0
29	25.1	37.1	22	17	22	18	0	−6
30	12.7	15.1	13	10	12	9	8	11
32	26.6	23.2	6	25	6	23	0	8
33	61.2	74.4	9	10	10	12	−11	−18
34	28.8	19.3	3	2	3	2	0	0
35	17.7	61.6	69	56	63	63	9	−12
36	40.2	29.1	19	22	20	22	−5	0
38	24.4	18.7	8	6	8	6	0	0
39	64.2	71.9	24	25	27	29	−12	−15
41	60.9	61.6	37	39	41	44	−10	−12
42	60.9	31.4	7	17	8	17	−13	0
43	26.0	22.6	12	4	12	4	0	0
44	14.4	17.5	2	15	2	14	0	7
45	60.9	40.7	25	15	27	16	−8	−6
46	21.1	40.7	27	26	25	26	8	0
47	32.3	37.1	10	13	10	14	0	−7
48	60.9	61.6	415	1212	463	1346	−11	−10
49	18.6	21.4	34	178	31	166	9	7
80	16.6	19.3	2	4	2	4	0	0
81	17.3	21.4	11	10	10	10	10	0
82	49.9	71.9	24	23	25	26	−4	−12
83	27.0	31.4	13	10	13	10	0	0
84	19.5	27.2	17	7	16	7	6	0
85	21.1	57.4	6	7	6	8	0	−13
86	18.1	21.4	21	36	20	33	5	9
Mean	33.4	39.6	134	76	139	82	4	7

[a]The first flux (J_{CO_2}) values are calculated using permeability values reported; the second flux values are calculated using the mean permeability value of the surveyed area (37 μm^2). Furthermore, the differences δ between the fluxes corrected for the measured permeability and those corrected for the mean permeability of the investigated area are also reported.

was assessed by using the coefficient of variation (CV), which is the standard deviation of the measurements divided by their arithmetic average and reported as a percentage; the CV values obtained for each site were lower than 5%. This value indicates that the flux measurements performed with this method are characterized by a good reproducibility.

4.6. Field Applications

[27] Two surveys of both soil CO_2 flux and soil permeability measurements were performed on Vulcano (Aeolian archipelago, Italy) in April and June 2003. The island is an active volcano which last erupted in 1888–1890 and, at the present, is characterized by solphataric activity. The explored area (Figure 11) covers about 2.2 km^2 and it is located on the western flank of La Fossa cone, between the isthmus of Vulcanello (to the north) and Grotta dei Palizzi (to the south).

[28] Soil permeability and flux measurements were performed in 48 fixed measurement sites where, since 1984, soil CO_2 flux measurements are periodically carried out for

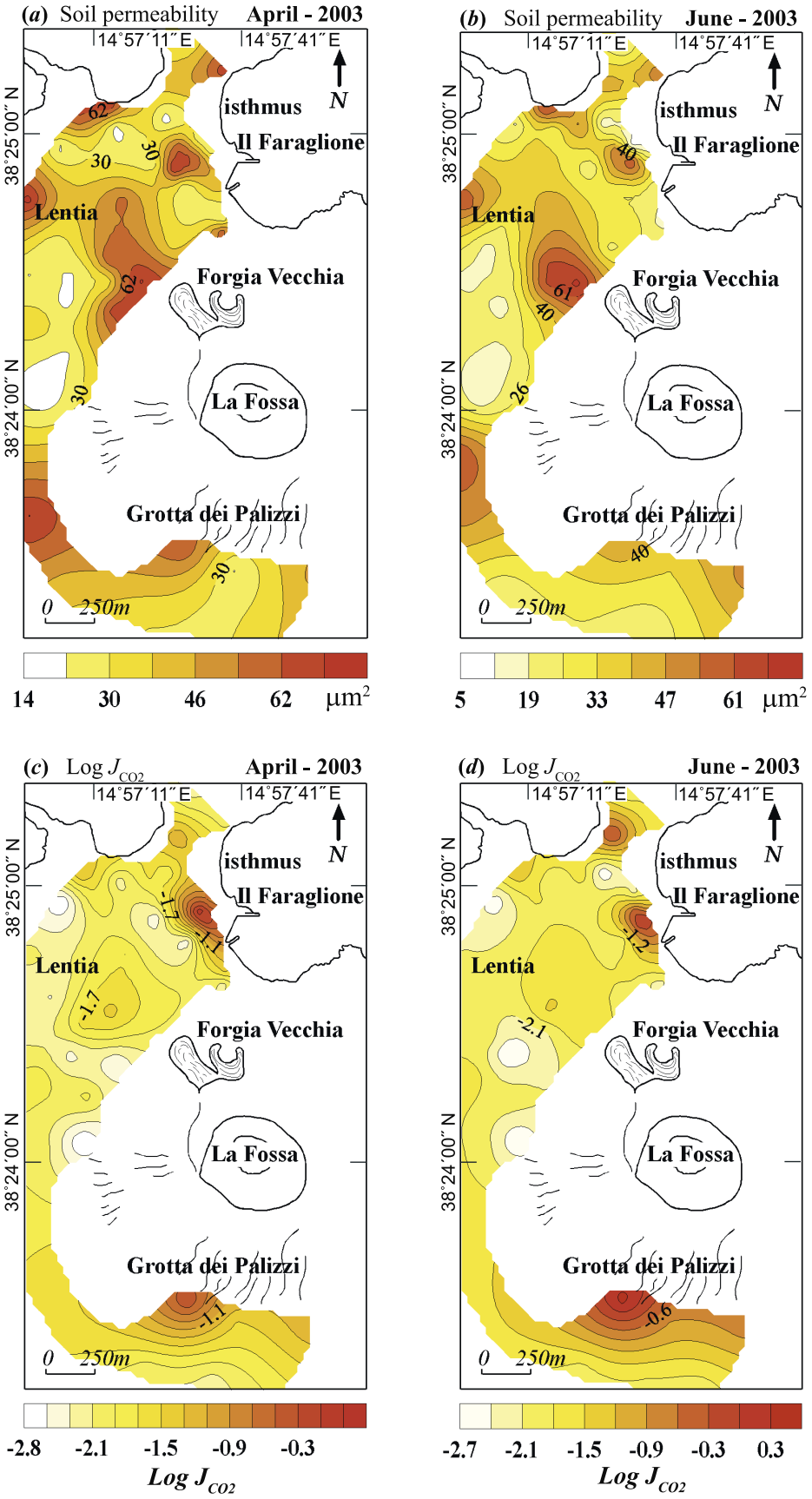

Figure 12. Spatial distributions of (a and b) the soil permeability and (c and d) CO_2 flux measured in the surveyed area of Vulcano Island, in April and June 2003, respectively.

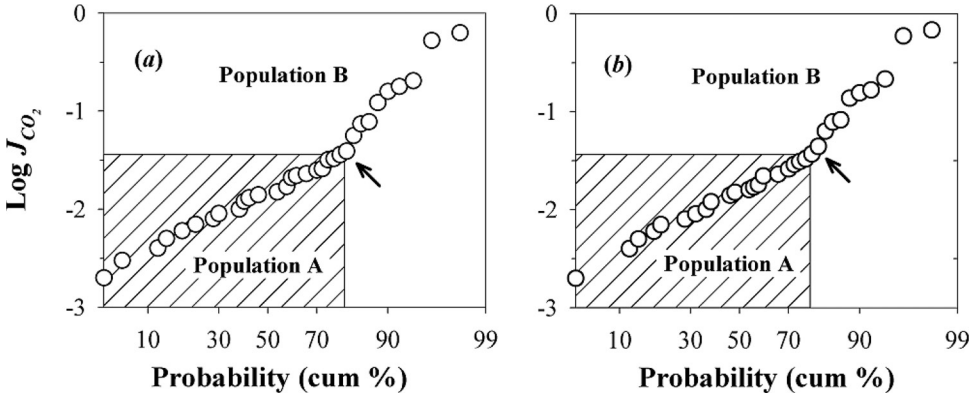

Figure 13. Cumulative frequency plot of the soil CO_2 fluxes relating to the April survey with (a) flux values corrected for the soil permeability measured in each site and (b) flux values computed using the mean permeability value of the surveyed area (37 μm^2).

volcanic surveillance purposes [*Badalamenti et al.*, 1988; *Diliberto et al.*, 2002].

[29] The gas permeability was measured in situ by the radial advection method [*Camarda et al.*, 2006]. These measurements were performed using a special probe which generates a gas source at a depth of 0.5 m and it permits measurement of the relative induced pressure in nearby soil at different depths. The gas permeability was computed according to the following equation:

$$\varphi_{r=R_1} = \frac{2k\pi}{\mu} \frac{R_1 R_2}{R_1 - R_2} \frac{\left(P_2^2 - P_1^2\right)}{P_1}$$

which predicts the gas flux crossing a spherical shell of radius R_1, when a radial and continuous gas source is generated in a porous medium of permeability k and the gas pressure at R_1 and R_2 radii is equal to P_1 and P_2, respectively.

[30] The flux measurements were performed exactly in the same site as the permeability measurements, using the dynamic concentration method and setting a value of pumping flux of 0.8 L min^{-1}. As generally made in the fumarolic gas sampling, before the introduction of the measuring probe into the soil, a cylindrical metal bar was inserted inside the probe. This prevents the occurrence of random occlusions of the gas inlets. The soil fluxes were calculated by equation (8) and the results are shown in Table 4. The measured permeability and flux values range from between 5 and 74 μm^2 and from 2×10^{-3} to 2.8×10^{-3} kg m^{-2} d^{-1}.

[31] The maps of Figure 12 show the spatial distribution of the soil permeability (Figures 12a and 12b) and the CO_2 flux (Figures 12c and 12d), measured in the surveyed area of the island of Vulcano, in the April and June surveys. The most permeable areas are located close to the Forgia Vecchia, the Lentia and Il Faraglione areas. The highest CO_2 fluxes for both the April and June surveys were located in the areas of Grotta dei Palizzi and Faraglione, while lower fluxes were recorded in the areas to the north of the Grotta dei Palizzi and the area close to the Lentia. Flux and permeability maps show that high soil CO_2 fluxes are located both in low and high permeability areas. This result suggests that the permeability of the upper soil layers have a negligible influence on the spatial distribution of diffuse soil gas emissions.

[32] Figure 13a shows the cumulative frequencies (expressed in probability scale) of the CO_2 flux values measured in the selected area in April 2003. In these kinds of plots [*Sinclair*, 1974], changes in slope are indicative of separate populations of data with lognormal distributions. The presence of an inflection point at the 72% cumulative percentile allows us to distinguish two populations of data with a lognormal distribution: a low flux population *A*, representing 72% of the entire data set, and an anomalous flux population *B*, representing 28% of the entire data. In Figure 13b, a similar plot of the flux data relating to the April survey has been reported. Figure 13b differs from Figure 13a because the plotted flux data have been calculated using equation (8) and a constant value of permeability for each site, which was set equal to 37 μm^2 (the mean permeability value found in the surveyed area). The results of these flux calculations have also been reported in Table 4 for both the April and June surveys, together with the difference (δ), expressed as a percentage between these values and those (fourth and fifth column) corrected for the permeability of each site. As shown in Table 4, δ value is always lower than 20%, with a mean value equal to 4% and 7% for the April and June surveys, respectively. Moreover, Figure 13 shows that although an error was made when calculating the CO_2 flux using an equal value of permeability for each site, this error was not large enough to cause any significant changes in the statistical distribution of the calculated soil CO_2 fluxes.

5. Conclusions

[33] The influence of soil permeability and pumping flux on soil CO_2 flux measurements, which were performed using the dynamic method [*Gurrieri and Valenza*, 1988], were investigated by means of several laboratory experiments and field investigations. An acceptable compromise in reducing response time and error in the flux measurements was achieved by setting a pumping flux of 0.8 L min^{-1}. In this case, a new empirical equation was deduced in order to include soil permeability in flux measurements. Very accurate measurements for soil CO_2

flux can be performed by applying this equation and measuring in situ soil gas permeability and the value of dynamic concentrations.

[34] Several in situ soil gas permeability measurements were performed using the radial advection method [*Camarda et al.*, 2006] over a large sector of the island of Vulcano (Aeolian Islands, Italy), the results of which identified a range of values of between 4 and 80 μm^2. The permeability values were compared with the soil CO_2 fluxes which had been measured at the same site at the same time using the dynamic concentration method, according to the new empirical equation, as deduced in this study. A low correlation between these two parameters was obtained, confirming the low importance of the permeability of the upper layers of the soil in determining the spatial distribution of soil gas emissions. Moreover, for each site of the surveyed area, CO_2 flux was also calculated by utilizing a single value of soil permeability, which was set equal to the mean value of permeability for the area under investigation. The error committed in this case was generally low and it did not cause significant changes in the statistical distribution of soil CO_2 flux.

Appendix A: Solution of Steady State Advective-Diffusion Equation

[35] The general solution of the steady state one-dimensional form of the advective-diffusion equation is [*Isachenko et al.*, 1980]

$$C(z) = A\frac{D}{v}e^{(v/D)z} + B \tag{A1}$$

where the A and B constants are calculated as a function of the boundary conditions.

[36] In order to describe the change in CO_2 concentration as a function of depth in a finite porous medium of thickness L, the following boundary conditions have been adopted:

$$C(z=0) = C_0$$

$$C(z=L) = C_L$$

where C_L and C_0 are the concentrations of gas at 0 and L depths, respectively. Under these conditions, the expression for the constants A and B can be easily found:

$$A = \frac{v}{D}(C_L - C_0)\left(e^{(v/D)z} - 1\right)$$
$$B = C_0 - (C_L - C_0)\left(e^{(v/D)z} - 1\right)$$

Replacing A and B terms in (A1), equation (6) is obtained:

$$C(z) = C_0 + \frac{(C_L - C_0)}{\left(\exp\left(\frac{v}{D}L\right) - 1\right)}\left(\exp\left(\frac{v}{D}z\right) - 1\right)$$

[37] **Acknowledgments.** This work was supported by the European Social Fund and the Department of Civil Protection. The authors wish to thank the Associate Editor and the two anonymous reviewers for their useful comments and suggestions.

References

Allard, P., et al. (1991), Eruptive and diffuse emission of CO_2 from Mount Etna, *Nature*, *351*, 387–391.

Anderson, J. M. (1973), Carbon dioxide evolution from two temperate deciduous woodland soils, *J. Appl. Ecol.*, *10*, 361–378.

Badalamenti, B., S. Gurrieri, S. Hauser, and M. Valenza (1988), Ground CO_2 output in the island of Vulcano during the period 1984–1988: Gas hazard and volcanic activity surveillance implications, *Rend. Soc. Ital. Mineral. Petrol.*, *43*, 893–899.

Badalamenti, B., S. Gurrieri, P. M. Nuccio, and M. Valenza (1991), Gas hazard on Vulcano island, *Nature*, *350*, 26–27.

Baubron, J. C., P. Allard, and J. P. Toutain (1990), Diffuse volcanic emissions of carbon dioxide from Vulcano island, Italy, *Nature*, *344*, 51–53.

Bekku, Y., H. Koizumi, T. Nakadai, and H. Iwaki (1955), Measurement of soil respiration using close chamber method: An IRGA technique, *Ecol. Res.*, *10*, 369–373.

Camarda, M., S. Gurrieri, and M. Valenza (2006), In situ permeability measurements based on a radial gas advection model: Relationships between soil permeability and diffuse CO_2 degassing in volcanic areas, *Pure Appl. Geophys.*, in press.

Campbell, G. S. (Eds.) (1985), *Soil Physics With Basic: Transport Models for Soil-Plant Systems*, 150 pp., Elsevier, New York.

Chiodini, G., and F. Frondini (2001), Carbon dioxide degassing from Albani Hillis volcanic region, central Italy, *Chem. Geol.*, *177*, 67–83.

Chiodini, G., R. Cioni, M. Guidi, L. Marini, and B. Raco (1998), Soil CO_2 flux measurements in volcanic and geothermal areas, *Appl. Geochem.*, *13*, 543–552.

Ciotoli, G., M. Guerra, S. Lombardi, and E. Vittori (1998), Soil gas survey for tracing seismogenic faults: A case-study in the Fucino basin (central Italy), *J. Geophys. Res.*, *103*, 23,781–23,794.

Ciotoli, G., M. Della Seta, M. Del Monte, P. Fredi, S. Lombardi, E. L. Palmieri, and F. Pugliese (2003), Morphological and geochemical evidence of neotectonics in the volcanic area of Monti Vulsini (Latium, Italy), *Q. Inter.*, *101–102*, 103–113.

De Gregorio, S., I. S. Diliberto, S. Giammanco, S. Gurrieri, and M. Valenza (2002), Tectonic control over large-scale diffuse degassing in eastern Sicily (Italy), *Geofluids*, *2*, 273–284.

Diliberto, I. S., S. Gurrieri, and M. Valenza (1993), Vulcano: Gas geochemistry. CO_2 flux from the ground, *Acta Vulcanol.*, *3*, 272–273.

Diliberto, I. S., S. Gurrieri, and M. Valenza (2002), Relationships between diffuse CO_2 emissions and volcanic activity on the island of Vulcano (Aeolian Island, Italy) during the period 1984–1994, *Bull. Volcanol.*, *64*, 219–228.

Evans, D. D., and D. Kirkham (1949), Measurement of the air permeability of soil in situ, *Soil. Sci. Soc. Am. Proc.*, *14*, 65–73.

Fang, C., and J. B. Moncrieff (1999), A model for soil CO_2 production and transport 1: Model development, *Agric. Forest. Meteorol.*, *95*, 225–236.

Gerlach, T. M., M. P. Doukas, K. A. McGee, and R. Kessler (2001), Soil efflux and total emission rates of magmatic CO_2 at the Horseshoe Lake tree kill, Mammoth Mountain, California, 1995–1999, *Chem. Geol.*, *177*, 101–116.

Giammanco, S., S. Gurrieri, and M. Valenza (1995), Soil CO_2 degassing on Mt. Etna (Sicily) during the period 1989–1993: Discrimination between climatic and volcanic influences, *Bull. Volcanol.*, *57*, 52–60.

Giammanco, S., S. Gurrieri, and M. Valenza (1998), Anomalous soil CO_2 degassing in relation to faults and eruptive fissure on Mount Etna (Sicily, Italy), *Bull. Volcanol.*, *60*, 252–259.

Grover, B. L. (1955), Simplified air permeameters for soil in place, *Soil Sci. Soc. Am. Proc.*, *19*, 414–418.

Guerra, M., and S. Lombardi (2001), Soil-gas method for tracing neotectonic faults in clay basins: The Pisticci field (southern Italy), *Tectonophysics*, *339*, 511–522.

Gurrieri, S., and M. Valenza (1988), Gas transport in natural porous medium: a method for measuring soil CO_2 flows from the ground in volcanic and geothermal areas, *Rend. Soc. Ital. Mineral. Petrol.*, *43*, 1151–1158.

Isachenko, V., V. Osipova, and A. Sukomel (Eds.) (1980), *Heat Transfer*, 493 pp. Mir, Moscow.

Kirita, H. (1971), Re-examination of the absorption method of measuring soil respiration under field conditions. IV. An improved absorption method using a disc of plastic sponge as absorbent holder, *Jpn. J. Ecol.*, *21*, 119–127.

Klinkenberg, L. J. (1941), The permeability of porous media to liquids and gases, *Drilling and Production Practices*, pp. 200–213, Am. Phys. Inst., College Park, Md.

Lunderghard, H. (1927), Carbon dioxide evolution of soil and crop growth, *J. Soil Sci.*, *23*, 417–454.

Millington, R. J., and R. C. Shearer (1971), Diffusion in aggregate porous media, *Soil Sci.*, *111*, 372–378.

Monteith, J. L., G. Szeicz, and K. Yabuki (1964), Crop photosynthesis and the flux of carbon dioxide below the canopy, *J. Appl. Ecol.*, *1*, 321–327.

Nakadai, T., H. Koizumi, Y. Usami, M. Satoh, and T. Oikawa (1993), Examination of the methods for measuring soil respiration in cultivated land: Effect of carbon dioxide concentration on soil respiration, *Ecol. Res.*, *8*, 65–71.

Natale, G., P. Hernández, T. Mori, and K. Notsu (2000), Pressure gradient measurements in volcanic diffuse gas emanations, *Geophys. Res. Lett.*, *27*, 3985–3987.

Norman, J. M., R. Garcia, and S. B. Verma (1992), Soil surface CO_2 fluxes and the carbon budget of a grassland, *J. Geophys. Res.*, *97*, 18,845–18,853.

Rogie, J. D., D. M. Kerrick, M. L. Sorey, G. Chiodini, and D. L. Galloway (2001), Dynamics of carbon dioxide emission at Mammoth Mountain Continuous monitoring of diffuse CO_2 degassing, Horseshoe Lake, Mammoth Mountain, California, *Earth Planet. Sci. Lett.*, *188*, 531–541.

Sahimi, M., (Eds.) (1995), *Flow and Transport in Porous Media and Fractured Rock: From Classical Methods to Modern Approaches*, 223 pp., VCH, New York.

Salazar, J. M. L., et al. (2002), Precursory diffuse carbon dioxide degassing signature related to a 5.1 magnitude earthquake in El Salvador, Central America, *Earth Planet. Sci. Lett.*, *205*, 81–89.

Scheidegger, A. E. (Eds.) (1974), *The Physics of Flow Through Porous Media*, 3rd ed., 353 pp., Univ. of Toronto Press, Toronto, Ont., Canada.

Sinclair, A. J. (1974), Selection of threshold values in geochemical data using probability graphs, *J. Geochem. Explor.*, *3*, 129–149.

Spicák, A., and J. Horálek (2001), Possible role of fluids in the process of earthquakes swarm generation in the West Bohemia/Vogtland seismoactive region, *Tectonophysics*, *336*, 151–161.

Tonani, F., and G. Miele (1991), Methods for measuring flow of carbon dioxide through soils in the volcanic setting, paper presented at International Conference Active Volcanoes and Risk Mitigation, IAVCEI, Naples, Italy, 27 Aug. to 1 Sept.

Wakita, H. (1996), Geochemical challenge to earthquake prediction, *Proc. Natl. Acad. Sci. U.S.A.*, *93*, 3781–3786.

Wentworth, C. K. (1922), A scale of grade and class terms for clastic sediments, *J. Geol.*, *30*, 377–392.

Witkamp, M. (1966), Decomposition of leaf litter in relation to environment, microflora and microbial respiration, *Ecology*, *47*, 194–201.

Witkamp, M., and M. L. Frank (1969), Evolution of CO_2 from litter, humus, and subsoil of a pine stand, *Pedobiology*, *9*, 358–365.

M. Camarda and S. Gurrieri, Istituto Nazionale di Geofisica e Vulcanologia, Sezione di Palermo, Via Ugo La Malfa 153, I-90146 Palermo, Italy. (m.camarda@pa.ingv.it)

M. Valenza, Dipartimento di Chimica e Fisica della Terra ed Applicazioni, Via Archirafi, 36, I-90136 Palermo, Italy.